Ingeniería Ambiental

Revista Mexicana de Ingeniería Química
Vol. 13, No. 3 (2014) 865-885

EFFECT OF THE FLUIDIZED BED DRYING ON THE STRUCTURE AND BIOSORPTION CAPABILITY OF Pb^{+2} OF AGAVE EPIDERMIS

EFECTO DEL SECADO POR LECHO FLUIDIZADO EN LA ESTRUCTURA Y CAPACIDAD DE BIOSORCIÓN DE Pb^{+2} DE EPIDERMIS DE AGAVE

M.T. Hernández-Botello[1], J.J. Chanona-Pérez[1*], J.A. Mendoza-Pérez[2], M. Trejo-Valdez[3], G. Calderón-Domínguez[1], J.L. Barriada Pereira[4], M.E. Sastre de Vicente[4], M.J. Perea-Flores[5], E. Terres-Rojas[6]

[1]*Departamento de Ingeniería Bioquímica,* [2] *Departamento de Ingeniería en Sistemas Ambientales ENCB,*
[3]*ESIQIE, IPN, México, D.F.*
[4]*Departamento de Química Física e Enxeñería Química I, Universidade da Coruña, Coruña, Spain.*
[5]*Centro de Nanociencias y Micro y Nanotecnologías, IPN, México, D.F.*
[6]*Laboratorio de Microscopia Electrónica de Ultra Alta Resolución, IMP, México D.F.*

Received May 29, 2014; Accepted June 23, 2014

Abstract

A fluidized bed drying study of agave epidermis obtained from wastes of the "pulque" manufacture was made. Drying kinetics modeling and the influence of the operation conditions on the shrinkage, microstructure and biosorption capability of Pb^{+2} were studied. Drying kinetics was carried out at 50, 60, 70 and 80 °C. Six semi-empirical models were tested and diffusion approach model provided the best fits. Effective diffusivity varied from 3.73×10^{-9} to 6.99×10^{-9} m^2s^{-1}, for untreated slabs (UT) and from 3.65×10^{-9} to 7.74×10^{-9} m^2s^{-1} for treated samples (T) with hydrochloric acid. Activation energy was found to be 21.22 and 23.89 kJ/mol for UT and T samples respectively. Shrinkage and the microstructure changes of T slabs were larger than UT samples. T samples dried at 70 and 80 °C showed a reduction in their Pb^{+2} biosorption capability, caused by a large shrinkage and severe microstructural changes. For UT samples their biosorption capability was increased in relation with increase of the shrinkage and drying temperature. T samples dried at 50 and 60 °C improved their biosorption capability of Pb^{+2}, while UT samples dried at 70 and 80 °C showed a better biosorption capability. These results can be useful for preparation of biosorbents.

Keywords: Agave epidermis, fluidized bed drying, shrinkage, microstructure, biosorption.

Resumen

Se realizó un estudio de secado en lecho fluidizado de epidermis de agave obtenida de desechos de la fabricación del "pulque". Se efectuó el modelado de las cinéticas de secado y se estudió la influencia de las condiciones de operación sobre el encogimiento, microestructura y capacidad de biosorción de Pb^{+2}. Las cinéticas fueron hechas a 50, 60, 70 y 80 °C. Seis modelos semi-empíricos fueron probados y el de aproximación a la difusión proporcionó los mejores ajustes. La difusividad efectiva cambio desde 3.73×10^{-9} a 6.99×10^{-9} m^2s^{-1} para las placas sin tratar, y desde 3.65×10^{-9} a 7.74×10^{-9} m^2s^{-1} para las muestras tratadas con ácido clorhídrico. La energía de activación fue de 21.22 kJ/mol para las muestras sin tratar y 23.89 kJ/mol para las muestras tratadas. El encogimiento y los cambios microestructurales fueron más drásticos en las placas tratadas en comparación con las rebanadas sin tratamiento ácido. El material tratado y secados a 70 y 80 °C, mostró una reducción en su capacidad de biosorción de Pb^{+2}, que fue causado por los cambios microestructurales y un encogimiento severo. Para la muestras sin tratamiento su capacidad de biosorción se incrementó con el encogimiento y la temperatura de secado. Las muestras tratadas y secadas a 50 y 60 °C, mejoraron su capacidad de biosorción. Estos resultados pueden ser útiles para la preparación de biosorbentes.

Palabras clave: epidermis de agave, secado por lecho fluidizado, encogimiento, microestructura, biosorción.

*Corresponding author. *E-mail*: jorge_ chanona@hotmail.com

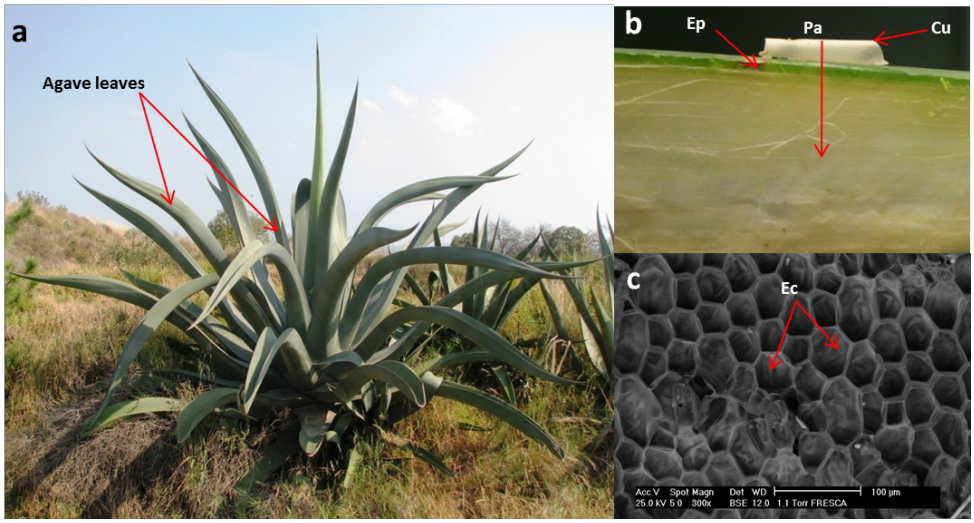

Fig.1. Parts of agave plant. a) Agave plant (*Agave atrovirens* Karw) , b) Cross section of agave leave: Epidermis (Ep), cuticle (Cu), parenchyma tissue (Pa) and c) Microphotograph of Agave epidermis tissue obtained by environmental scanning electron microscopy, shows epidermis cells (Ec).

1 Introduction

The exploitation of the most important species of agave in Mexico (*Agave tequilana* Weber, *A. americana* and *A. atrovirens* Karw) generates an extensive quantity of agroindustrial wastes derived mainly from production of "tequila", "mezcal" and "pulque". It is estimated that about 350 000 tons per year of agroindustrial residues are generated in the mezcal industry in Mexico. Agave wastes cause complications for its final disposal due to its high humidity level (>80 % d.b.) causing a slow decomposition and a great waste volume. Leaves and agave pulp (Figure 1a and 1b) are the remaining biomass in the extraction of polysaccharides and syrups; which are used in the production of alcoholic drinks. The bagasse is mainly constituted by parenchymal, vascular tissue and epidermis of the plant. Bagasse is commonly used for the production of traditional products such as textile weaving, paper pulps, glues, food for cattle and other craft uses and recently is considered as a potential source of lingocellulosic material for the manufacture of low-cost composites (Bessadok *et al*., 2009). About 54% of the agave total weight corresponds to the head that is mainly used to produce tequila and other liquors. The leaves represent 32% and have been used for the production of sugar and fibers; whereas the remaining 14% includes the epidermis and the cuticle (Figure 1b), that do not have any important use (Iñiguez *et al*., 2001). The epidermis is the outermost layer of plant cells (Figure 1b); this layer is in direct contact with the environment and it is responsible of important functions such as gases change, water vapor, water storage, photosynthesis, support and mechanical protection. The agave epidermis contains cellulose, hemicellulose, lignin, silica, oils, salts in crystalline form, resins and a cuticle with waxes monostratified and stomata on both sides of the leaf. Epidermal tissue is constituted by cortical parenchyma cells (Figure 1c), abundant chloroplasts and mucilage cells with high content of polysaccharides that confer to the epidermis a large water absorption capability. The epidermis cell wall has an anionic character due to the presence of polar functional groups such as carboxyl, hydroxyl, phosphate and sulfide, which contribute to the formation of ionic interchange sites. Some reports had considered the potential of agave wastes as biosorbent to purify polluted effluents with heavy metals, polar compounds and dyes (Romero *et al*., 2005; Velazquez *et al*., 2013). For this reason, it is necessary to find an alternative use for this agroindustrial waste. Often, biosorbents obtained from agroindustrial waste are chemically activated by immersion in acid solutions (HCl or HNO_3) with the purpose of increasing its biosorption capability. After the chemical activation, they are dried in order to remove the water excess to facilitate its handling and

storage (Qi and Aldrich 2008; Mata *et al*., 2009; Schiewer and Balaria, 2009; Feng *et al*., 2011).

Other important issue for preparation of biosorbents is the drying, this is one of the oldest techniques used for the preservation of agricultural products since this technology prevents microbial deterioration and offers lighter weight and smaller volume for the transportation and storage. Drying of biomaterials involves physical and chemical changes which dramatically affect the products itself and its final properties, as well as its functionality such as adsorption capability of water and chemical compounds (Senadeera *et al*., 2003). Among the drying technologies, the fluidized bed drying is widely used to dry powders, grains and small pieces of vegetable tissues due to its higher heat and mass transfer coefficients. Additionally, fluidized bed drying provides a more homogenous product than conventional or solar drying (Doymaz, 2005; Demir *et al*., 2007; Arabhosseini *et al*., 2009; Akmel *et al*., 2009; Perea *et al*., 2012).

The drying kinetics studies are essential to evaluate drying rates and effective moisture diffusivity (Vagenas and Karathanos, 1993; Perea *et al*., 2012). These can be reproduced by using models (transfer coefficients and drying constants) that are directly related to the drying conditions and describe the phenomenon in a simplified way. Such models are commonly used in order to estimate drying times of the materials and also to generalize drying curves (Doymaz, 2005; Demir *et al*., 2007; Arabhosseini *et al*., 2009; Akmel *et al*., 2009). In order to study the drying effect on the biomaterials, it is necessary a deep knowledge of the mass transfer parameters and drying kinetics modelling which are considered important for the design, the selection of optimal drying conditions, quality control of the biomaterials, simulation and optimization of the drying process (Guine and Fernández, 2006). The mathematical models have proved to be very useful in the new design and/or improvement of drying systems, and for the analysis of mass transfer phenomena involved during drying. Thus, it is necessary to find accurate models, capable of predicting the water removal rates and describing the drying performance of each biomaterial under the common conditions used in the industrial processes (Perea *et al*., 2012; Doymaz, 2005). Nevertheless, there are few studies related with the drying of agro-industrial wastes and the modeling of its drying kinetics, such as the epidermis of *A. atrovirens* (Doymaz, 2005; Demir *et al*., 2007; Arabhosseini *et al*., 2009; Akmel *et al*., 2009; Perea *et al*., 2012). Considering this background and which there are not enough data available in the literature about the drying of agave epidermis and its effect on the biosorption of heavy metals, the leading objectives of this work can be summarized as follows:

To characterize the drying of agave epidermis untreated (UT) and treated (T) with hydrochloric acid solution through drying parameters such as effective moisture diffusivity coefficients, activation energy as well as the mathematical modeling of drying kinetics. To study the relationships between drying conditions, shrinkage, microstructure and biosorption capability of Pb^{+2}.

2 Material and methods

2.1 Sample preparation

Agave epidermis was obtained from waste of agave leaves (*A. atrovirens*) remnant of handcraft elaboration of a local beverage ("pulque"). Agave leaves were collected from 5-7 years old plants from a plantation established in México City. Agave leaves were washed with distilled water and the cuticle was removed manually. Epidermis slabs of approximately 0.6 × 0.6 × 0.4 cm were obtained by manual cutting. Two types of samples were used, untreated slabs (UT) were soaked in distilled water and other slabs were treated (T) with 0.1 M hydrochloric acid (1:250w/v) to protonated the surface of the samples. This treatment is usually applied in biological samples for active its surface and improve the biosorption of heavy metals (Qi and Adrich, 2008; Schiewer and Balaria, 2009). Both samples were stirred in glass flasks at 250 rpm during 30 min at 25 ºC. The samples were extensively washed with milli-Q water (Millipore Direct-Q 3, USA) until the pH of the suspension reached 5.0. Then, UT and T samples were pressed against a filter paper in order to remove the remaining water (Bhainsa and D'Souza, 2008). Initial moisture content of the samples (UT and T) was determined according to the Association of Official Analytical Chemists (AOAC) 32.1.03 method. All measurements were performed in triplicate. This moisture content was used as the initial moisture content in the drying kinetics.

2.2 Drying experiments

Drying experiments were carried out in a fluidized bed dryer at laboratory scale (ArmfieldFT31, UK). The drying column (section test) was made of an acrylic cylinder (9.6 cm internal diameter, 35 cm

height). Epidermis slabs were dried at different air temperatures (50 ºC, 60 ºC, 70 ºC and 80 ºC) and air flow was kept constant (2.3±0.2 m s^{-1}) for all drying condition. Pressure drop measurements for the fluidized bed were obtained using U-tube manometer filled with distillate water. Under this regime of air flow a good fluidization was obtained and the bed material showed a perfect mixing. The pressure drop in the packing bed material showed almost no fluctuations as the air flow was increased, which was a measurement for smooth fluidization without slug formation, which is an adequate fluidization according to reported by Gazor and Mohsenimanesh (2010). A thermoanemometer (TSI Inc, 8330-M, USA, accuracy of ±0.1 m/s) was used for monitoring the dry bulb temperature and air velocity. Wet bulb temperature was measured by means of type-K-thermocouple wrapped in a distillate water wet cotton cloth and connected to a digital thermometer (Dakota Instruments Inc, 1604, USA, accuracy of ±0.1 °C). Changes in the absolute humidity of air at the inlet of the column were determined from the psychometric chart using wet and dry bulb temperatures. The absolute humidity of the drying air oscillated from 0.001 to 0.003 kg water/kg air dry at all studied temperatures. In the present work the influence of air temperature was the only parameter studied as it is considered in several reports as the key factor affecting drying kinetics. Furthermore, the selected temperature range (50-80 °C) used in this research is typical for the study of biological materials drying process (Sturm *et al*., 2014; Gumeta *et al*., 2011; Gazor and Mohsenimanesh *et al*., 2010; Doymaz, 2005). Each drying run was carried out to a specified mass of agave epidermis slabs (42 ± 0.5 g) measured with a digital balance (Adam equipment, PGW 4502i, USA, accuracy±0.01 g) and L/D ratio of 0.5, where L is the bed height (4.8±0.3 cm) and D is the bed diameter, as recommended by Santiago-Pineda *et al*., (2007). The height of the static bed was measured using a Vernier caliper (Mitutoyo, Kawasaki 39652-20, Japan). During drying experiments, the weight loss of the slabs was measured with the digital balance aforementioned, every 2 min until no further changes in their mass were observed (constant weight), taking less than 10 s to weigh the sample. Drying kinetics were calculated based on the initial and final mass, moisture content, weight loss, final moisture and the dried solid content of slabs, plotting the moisture ratio (MR, see equation 1) in function of drying time. The equilibrium moisture content of slabs was obtained by using the dynamic method described by Kashaninejad *et al*., (2007). The drying experiments were replicated three times and drying kinetics was reported as the average of the three replicates. An analysis of variance (ANOVA) and a Tukey test were applied in order to statistically compare the results between the drying kinetics replicates of both untreated and treated samples. The ANOVA also was used to compare the effect of drying temperature on the shrinkage and ion removal in both kind samples (UT and T); significant differences were considered when $p \leq 0.05$.For these analysis Sigma Plot software version 12.0 (SYSTAT Inc., USA) was used.

2.3 *Mathematical modeling of the drying kinetics*

To study the drying kinetics of agave epidermis slabs, it is important to select an accurately model for describe acceptably its drying behavior. Thus, in this work the experimental drying kinetics data for each of experiment were fitted to six of the most frequently semi-theoretical models, which were selected from recent researches focused in the drying of similar agricultural products (Shen *et al*., 2011; Promvonge *et al*., 2011; Doymaz, 2005). The models selected were: exponential or Lewis, Henderson and Pabis, Page, two-term exponential, logarithmic and diffusion approach or approximation of the diffusion. The mathematical expressions and relevant information about these models are shown in Table 1. In these models, the dimensionless moisture ratio (MR) of agave epidermis slabs during fluidized bed drying experiments was calculated from the following equation:

$$MR = \frac{M_t - M_e}{M_o - M_e} \tag{1}$$

where M_o is the initial moisture content, M_e is the equilibrium moisture content, and M_t is the moisture content at time t (Wang *et al*., 2007; Iguaz *et al*., 2003).

The drying rate (DR) expressed as g (water) g^{-1} (dry solids) min^{-1} is defined as:

$$DR = \frac{M_1 - M_2}{t_2 - t_1} \tag{2}$$

where t_1 and t_2 are the drying times in minutes at different times during fluidized bed drying; M_1 and M_2 are the moisture contents (d.b.) of agave slabs at time t_1 and t_2, respectively.

Table 1. Mathematical models selected to modelling of agave slabs drying kinetics

Models	Model equation	Model constants	Relevant information	References
Exponential or Lewis	$MR = \frac{M_t - M_e}{M_o - M_e} = \exp(-kt)$	k	This model assumes negligible internal resistance, which means that there is not resistance in the moisture displacement between the interior of material towards the material surface	Doymaz, (2005); Kashaninejad *et al.*, (2007); Perea *et al.* (2012).
Henderson and Pabis	$MR = \frac{M_t - M_e}{M_o - M_e} = a\exp(-kt)$	a, k	This model controls the liquid process diffusion and take place only in the falling rate period	Doymaz, (2005); Vega-Galvez *et al.*, (2010); Perea *et al.*, (2012).
Page	$MR = \frac{M_t - M_e}{M_o - M_e} = \exp(-kt^n)$	k, n	This model suggests the used of two empirical constants, it has been shown to produce good fits to describe drying of many agriculture products.	Iguaz *et al.*, (2003); Rafiee *et al.*, (2009); Perea *et al.*, (2012).
Two term exponential	$MR = \frac{M_t - M_e}{M_o - M_e} = a_1\exp(-k_1 t) + a_2\exp(-k_2 t)$	a_1, a_2, k_1, k_2	This model assumes that diffusivity is constant and solution applies regardless of particle geometry and boundary conditions.	Iguaz *et al.*, (2003); Rafiee *et al.*, (2009); Vega-Galvez *et al.*, (2010); Shen *et al.*, (2011).
Logarithmic	$MR = \frac{M_t - M_e}{M_o - M_e} = a\exp(-kt) + c$	a, k, c	This model has been successful used to fit drying kinetics at different operation conditions.	Demir *et al.*, (2007); Sacilik, (2007); Sirisomboon and Kitchaiya, (2009); Vega-Galvez *et al* (2010).
Diffusion approach or approximation of the diffusion	$MR = \frac{M_t - M_e}{M_o - M_e} = a\exp(-kt) + (1 - a)\exp(-kbt)$	a, k, b	This model tends to underestimated in the latter stage while the model tends to have a good fit in the initial stages for several drying conditions.	Akgun and Doymaz, (2005); Rafiee *et al.*, (2009); Perea *et al.*, (2012).

*t is the time for all equations

2.4 *Statistical evaluation of the mathematical models*

The statistical validity of models was evaluated and compared by means of different statistical indicators and the non-linear regression analysis of drying kinetics was done using SigmaPlot software version 12.0 (SYSTAT Inc. USA). The drying rate constants and coefficients of all models were estimated using non-linear least squares regression analysis, performed using Marguardt-Levenberg algorithm. In order to select the best model to describe drying behavior accurately, the coefficient of determination R^2, was used as the main+41 00 selection criteria,

but also the goodness of the fit was determined additionally using others statistical parameters such as reduced chi-square (χ^2), mean relative percent deviation (E_{MD}) and root mean square error (E_{RMS}) values. For quality fit, R^2 value should be higher and χ^2, E_{MD} and E_{RMS} values should be lower (Promvonge *et al*., 2011;Doymaz, 2011; Vega *et al*., 2010; Wang *et al*., 2007; Kashaninejad *et al*., 2007). The parameters were calculated using the following expressions:

$$R^2 = \sum_{i=1}^{N} \frac{M_{R,pre,i} - \bar{M}_{R,ex,i}}{(M_{R,ex,i} - \bar{M}_{R,ex,i})^2} \tag{3}$$

$$E_{MD} = \frac{100}{N} \sum_{i=1}^{N} \frac{|M_{R,ex,i} - M_{R,pre,i}|}{M_{R,ex,i}} \tag{4}$$

$$E_{RMS} = \left[\frac{1}{N} \sum_{i=1}^{N} \left(M_{R,ex,i} - M_{R,pre,i} \right)^2 \right]^{1/2} \tag{5}$$

$$\chi^2 = \frac{\sum_{i=1}^{N} \left(M_{R,ex,i} - M_{R,pre,i} \right)^2}{N - z} \tag{6}$$

where: $M_{R,exp,I}$ and $M_{R,pre,I}$ are experimental and predicted dimensionless moisture ratios, respectively; N is the number of observations; and z is the number of constants. E_{MD} (%) indicates the deviation between the experimental data and predicted data.

2.5 Estimation the effective moisture diffusivity (D_{eff}) and activation energy (E_a)

The effective moisture diffusivity of agave epidermis slabs was studied using the mathematical Fick's second diffusion model. The solution to this equation, developed by Crank (1975), could be used for various regularly shaped bodies such as slabs, cylindrical and spherical products. In this work the usage of the form of Eq. (7) could be applicable for samples with slab geometry by assuming uniform initial moisture distribution (Shen *et al*., 2011; Crank, 1975).

$$MR = \frac{8}{\pi^2} \sum_{n=0}^{\infty} \frac{1}{(2n+1)^2} - \left(\frac{(2n+1)^2 \pi^2 D_{eff} t}{4L^2} \right) \tag{7}$$

where MR is the moisture ratio, D_{eff} is the effective diffusivity (m^2s^{-1}) and L is the half thickness of slab (m) and t is the time (s). Slab thickness was calculated using an image analysis methodology similar to reported by Perea *et al*., (2011) and it is describe in detail in the following section. For long drying time, Eq. (7) could be further simplified to retain only the first term and the logarithmic form is showed in the Eq. (8). The effective moisture diffusivity could be typically determined by plotting experimental drying data in tE_{RMS} of ln(MR) *versus* drying time (Doymaz, 2011; Shen *et al*., 2011; Wang *et al*., 2007) and D_{eff} was calculated from slope of the plot.

$$\ln MR = \ln \frac{8}{\pi^2} - \left(\frac{\pi^2 D_{eff} t}{4b^2} \right) \tag{8}$$

The D_{eff} can be related to temperature of fluidized bed drying by Arrhenius equation (Promvonge *et al*., 2011; Wang *et al*., 2007; Iguaz *et al*., 2003) as show in the Eq. (9)

$$D_{eff} = D_o \exp\left(-\frac{E_a}{RT} \right) \tag{9}$$

where D_o is the pre-exponential factor equivalent to the diffusivity at infinitely high temperature (m^2s^{-1}), E_a is the activation energy ($kJmol^{-1}$), R is the universal gas constant (8.314 J $mol^{-1}K^{-1}$), and T is the absolute temperature (K). Both kinetic parameters (E_a and D_o) could be determined by plotting ln(D_{eff}) *versus* T^{-1} after linearization for Eq. (9) (Shen *et al*., 2011;Vega *et al*., 2010).

2.6 Shrinkage of agave slabs

Top and lateral views of samples were considered to evaluate the shrinkage of agave slabs. For the top view, the acquisition of images was carried out with a color digital camera (CCD) model power shot SX110 IS (Canon, NY, USA) with nine megapixels and positioned vertically over the sample at a distance of 15.5 cm from the floor of the computer vision system to the lens as previously reported (Arzate *et al*., 2012). The images were taken using the following camera settings: manual mode with lens aperture at f = 2.8 and speed 1/15 s, no zoom and no flash. A matte white background was used to improve the contrasts during the capture of this view. Due to small thickness of agave slabs and to avoid shadows, the lateral view images were obtained by using a stereomicroscope (Nikon SMZ 1500, Japan) and the samples were positioned laterally by using white play-dough to set up a vertical position and improve the contrast. The image capture procedure was similar to that reported by Perea *et al*. (2012). All images were captured as RGB and stored in BMP format to a size of 1600×1200 pixels. A reference bar in mm was positioned very close to the slabs in both captured scenes, thus the resolution of images was estimate in 0.0082 mm/px.

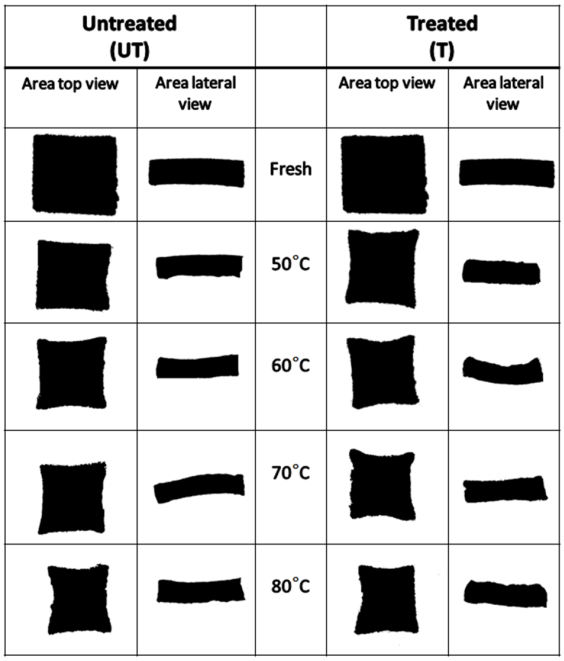

Fig. 2. Binary image gallery of agave epidermis slabs, top view and lateral view, as function of drying temperature, untreated and treated samples.

For both views around 600 images of agave slabs were used to evaluate the shrinkage by using projected area and thickness of slabs. Image processing included: cropping, conversion of the color image to grey-scale values, application of a threshold tool at grey level in a limited range from 0 to 85-110 units in the intensity histogram of pixels and background subtraction to obtaining the binary image from the grey-scale images. Subsequently, projected area and thickness of the images were obtained as number of pixels within the boundary (Figure 2). According with McLaughlin, and Magee, (1998) the shrinkage could be evaluated, assuming that this process is isotropic, and that the sample geometry corresponds to a rectangular parallelepiped. Under these assumptions, the slabs volume was estimate from project area of top view multiplied by the average slabs thickness of lateral view. The thickness was measured in different zones of the lateral views and at least 3 measurements were taken, one at the center and two at the slab tips. The shrinkage was expressed as a percentage of change or relative to the original geometry of the slabs. Thus, the relative shrinkage was estimated by using the following expression (Sansiribhan *et al*., 2012):

$$Shrinkage(\%) = \frac{V_i - V_f}{V_i} \times 100 \qquad (10)$$

where V_i is the initial volume obtained from images of fresh slabs and V_f is the final volume. The image analysis was selected as a methodology for evaluation of the shrinkage, because it has been used as successful method to estimate the shrinkage in the drying of biological materials (Fernandez *et al*., 2005; Gumeta *et al*., 2011).Around 300 images were used in the measurements for each view at initial and final drying time. ImageJ software v.1.48i (National Institutes of Health, Bethesda, MD, USA) was used in all steps of image analysis methodology.

2.7 *Environmental scanning electron microscopy (ESEM)*

To examine the microstructural changes caused by the drying process on the agave epidermis surface, the samples (fresh, dry, untreated and treated) were mounted on aluminum stubs with double-sided carbon adhesive tape and directly observed under a XL-30 Environmental Scanning Electron Microscope (Philips, USA) at 25 kV accelerating voltage. ESEM was coupled to a GSE (gaseous secondary electron detector).

2.8 *Biosorption capability of Pb^{+2}*

Biosorption experiments were carried out with fresh and dry UT and T agave slabs samples. In all cases, 0.7 g of material were mixed (175 rpm) at room temperature (25°C) with 20 mL of 100 ppm Pb^{+2} solution (pH 5, adjusted with diluted HNO_3 and NaOH) for 30 min. Pb^{+2} concentration was selected due to at this level, the precipitation of Pb^{+2}at the pH used was avoided, besides, this concentration conditions was in the suitable range used in the biosorption experiments reported by other authors (Qi and Aldrich, 2008; Schiewer and Balaria, 2009; Mata *et al*., 2009). After mixing, the samples were filtered (Whatman 40 filter paper), and the Pb^{+2} concentration of the filtrate was analyzed using the Polarographic (Metrohm polarographic analyzer, model 707, Switzerland) coupled to a personal computer. A typical three electrode system equipped with a dropping mercury working electrode, a platinum counter electrode and Ag/AgCl/3 M KCl as a reference electrode. Nitrogen was used as an inert gas to purge the analyze solution and to operate the mercury electrode. The optimum nitrogen gas pressure of 0.5 kg cm^{-2} was used throughout in this study (Comte, *et al*., 2008, 2006; Mohammadi *et al*., 2004). Relative biosorption capability of agave

slabs was expressed as ion removal (%) according to reported by López-Garcia *et al*., (2012) and it was obtained by means of following equation:

$$ion\ \ removal(\%) = \frac{c_i - c_f}{c_i} \times 100 \qquad (11)$$

where c_i is the initial concentration in the solution and c_f is the final concentration in the solution, estimated from a calibration curve of Pb^{+2} concentration (C) in ppm against current intensity (CI) in amperes (CI=0.224C+2.737, R^2=0.99, range of 0-200 ppm of Pb^{+2}). All experiments were replicated at least three times.

3 Results and discussion

3.1 Drying curves analysis

Initial moisture content of untreated (UT) and treated (T) agave slabs was in both cases of 86.6 ±0.5% (d.b.). The changes in MR as function of drying time of agave slabs at different air drying temperatures (50-80ºC) are presented in Figures 3a and 3b. The drying time required to reduce the moisture from initial moisture for UT agave slabs to final moisture content was 34, 28, 18 and 14 min at air drying temperatures of 50, 60, 70 and 80ºC, respectively. The final moisture contents reached for each time were 2.97 ±0.19, 1.16±0.24, 1.75±0.22 and 2.47± 0.19% d.b. respectively. In the case of T agave slabs, the drying time was 34, 28, 20 and 16 min at air drying temperatures of 50, 60, 70 and 80ºC, respectively. The final moisture contents (equilibrium moisture) reached for each time was 2.97 ±0.19, 2.85±0.19, 2.79 ±0.19 and 2.61±0.18% d.b. respectively. As expected the moisture ratio was reduced exponentially with drying time in both kinds of samples; this behavior is typical for the drying of some biological materials (Doymaz, 2005; Calzetta *et al*., 2004; Shen *et al*., 2011; Wang *et al*., 2007). The drying kinetics behavior suggests that the drying process occurs mainly during the falling rate period, and as consequence the drying rate is controlled by internal diffusion phenomenon, thereby molecular diffusion migration of the moisture contained in the samples could be the predominant mechanism for drying, as has been reported for several agricultural products (Doymaz, 2011; Gazor and Mohsenimanesh, 2010; Gumeta *et al*., 2011; Kashaminejad *et al*., 2007; Vega *et al*., 2010; Zielinska and Markowski, 2007).

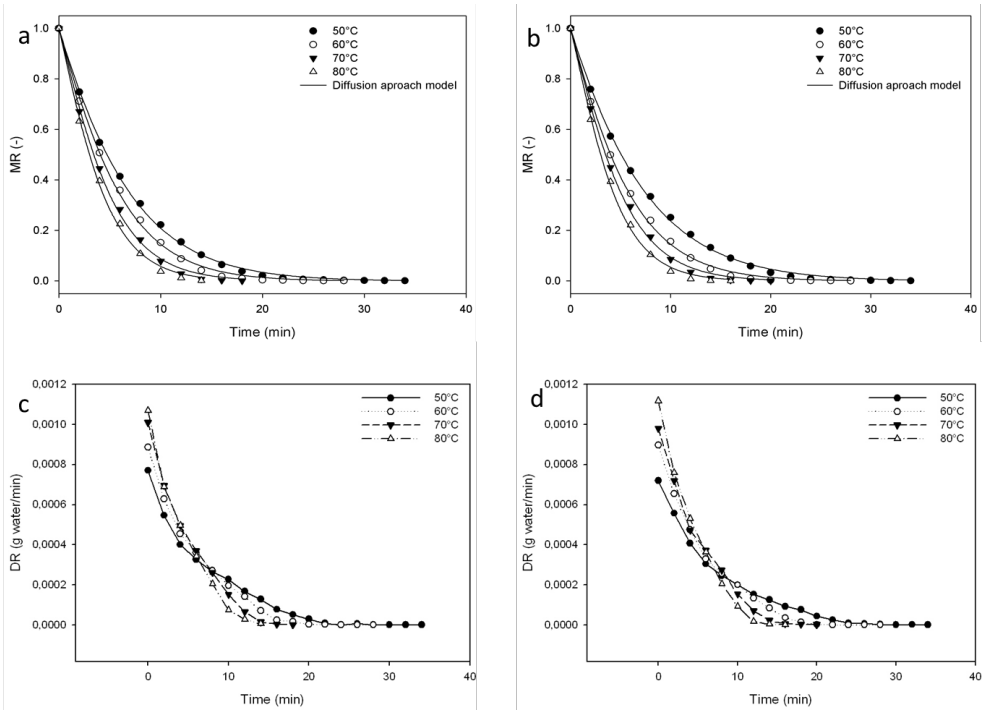

Fig. 3. Experimental and predicted moisture ratio (MR) by diffusion approach model in function drying time at different drying temperatures for agave slabs, a) untreated and b) treated. Experimental drying rate (DR) curves at different drying temperatures for agave slabs, c) untreated and d) treated.

The statistical analysis (ANOVA) of the drying kinetics revealed that there is no significant difference ($p < 0.05$) among untreated and treated slabs, when the drying is carried out at the same temperature. Nevertheless, for both kind of samples the moisture ratio was increased with the increment of the drying air temperature and showed significant differences ($p < 0.05$) between the different drying temperatures applied. This effect is in agreement with other reports of drying for different vegetable tissues (Abalone *et al*., 2006; Arabhosseini *et al*., 2009; Barrozo *et al*., 2006; Chua *et al*., 2000; Doymaz, 2005; Kerdpiboon *et al*., 2007; Ruiz *et al*., 2008; Sacilik *et al*., 2006; Shivhare *et al*., 2000).

Additionally to the drying kinetic analysis, the amount of water removed from samples as function of time was represented as drying rate (DR). These curves, at the different tested drying temperatures (50, 60, 70 and 80ºC), are shown in Figure3c and 3d for UT and T agave slabs, respectively. The DR decreases continuously with drying time, and this behavior confirm that the drying process occurred mainly during the falling rate period. Also, when the air temperature was increased, the DR parameter increased too. Similar results related to behavior of DR curves have also been reported in several drying studies of biological materials (Doymaz, 2005; Calzetta *et al*., 2004; Shen *et al*., 2011; Wang *et al*., 2007).

3.2 Mathematical modeling of the drying kinetics

In the Tables 2 and 3, the details of the statistical analysis results for the six models applied to drying kinetics of UT and T agave slabs are shown. The values of R^2, E_{MD}, E_{RMS} and χ^2 changed between 0.9997-0.9964, 0.189-1.053, 0.0016-0.0280 and 0.000082-0.00148 respectively. R^2 values greater than 0.99 were found for the six models tested. It was observed that the diffusion approach and the logarithmic model showed higher R^2 values than the others models tested (Table 2 and 3), presenting the former a better performance (R^2) to fit curves than the logarithmic model. In contrast, the Lewis and Henderson and the Pabis models showed a minor fit to experimental drying data in comparison with logarithmic and diffusion approach models. Even though Lewis model is easier to implement than the others, because it uses only one fitting constant, the results indicated that Lewis and Henderson and Pabis models yielded lower values of R^2 and higher E_{MD} (%) than diffusion approach and logarithmic models. These results could be due to that Lewis model is a special case of the Henderson and Pabis model, but both models tended to overestimate in the early stages and underestimate in the later stages of the drying (Akgun and Doymaz, 2005). However, for all mathematical models E_{MD} (%) values were lower than 10%, and this level of bias is accepted as adequate. These results indicated that all models had low deviation in relation to experimental data and it is not surprising that the diffusion approach model showed the lowest values of E_{MD} (%) in almost all cases, except for agave slabs untreated at 70 and 80 °C, where the logarithmic model presented the lowest E_{MD} (%) values (Table 2). The analysis of E_{RMS} showed that the diffusion approach model give a superior fit to experimental data (Table 2 and 3). Also, diffusion approach model provided lower χ^2 values in comparison with the others models; when χ^2 values approach to zero, the closest is the prediction (Roberts *et al*., 2008; Gazor and Mohsenimanesh, 2010), which indicated good predictions to drying kinetics of UT and T agave slabs. Similar results have been reported for several agricultural products such as medicinal plants (*Gundelia tournefortii*, Evin, 2012), aromatic plants (tarragon, *Artemisa dracunculus*, Arabhosseini *et al*., 2009), apple (Wang *et al*., 2007), green beans (Doymaz, 2005) and coconut (Niamnuy and Devahastin, 2005).

In Figures 3a and 3b the experimental MR data fitted to the diffusion approach model is shown. It can be observed from this figure that there is a suitable fit between experimental and predicted MR data. Based on this statistical information, it is possible to select the diffusion approach model as the best for describing the behavior of fluidized bed drying of UT and T agave slabs. Diffusion approach model has also been reported by other authors as an adequate model to fit drying kinetics of several food materials such as okra (Doymaz, 2011), canola seeds (Gazor and Mohsenimanesh, 2010), rough rice (Cihan *et al*., 2007) and plum (Sacilik *et al*., 2006).

Additionally to the selection of an accurate model to describe the agave samples drying kinetics, a direct link between k coefficients and the air drying temperatures was established, observing a similar tendency to that showed in MR and DR curves; this can be noticed in Tables 2 and 3. The values of k can be related to the effective moisture diffusivity when the drying process is controlled by internal diffusion phenomena. Thereby, k values can be associated with the facility of moisture to be removed from the material.

Table 2.Statistical results obtained from the six selected drying models and estimate parameters for slabs agave slabs untreated

Temperature (°C)	Models	Model constants	R^2	EMD (%)	ERMS	χ^2
50	Henderson and Pabis	a:1.0147, k:0.1565	0.9976	0.3180	0.0135	0.00020
	Lewis	k:0.1544	0.9974	0.3290	0.0010	0.00021
	Page	k:0.1286, n:1.0862	0.9989	0.2150	0.0093	0.00009
	Two term exponential	a_1:0.5115, k_1:0.1565, a_2:0.5032,k_2:0.1565	0.9976	0.3180	0.0135	0.00023
	Logarithmic	a:1.0255, k:0.1473, c:-0.0193	0.9990	0.2020	0.0086	0.00008
	Diffusion approach	a:-121.8259, k:0.2182, b:0.9968	0.9991	0.1890	0.0082	0.00008
60	Henderson and Pabis	a:1.0201, k:0.1867	0.9955	0.5620	0.0199	0.00045
	Lewis	k:0.1834	0.9951	0.5704	0.0207	0.00046
	Page	k:0.1401, n:1.1380	0.9983	0.3040	0.0121	0.00017
	Two term exponential	a_1:0.5176, k_1:0.1867, a_2:0.5024, k_2:0.1867	0.9955	0.5620	0.0199	0.00054
	Logarithmic	a:1.0366, k:0.1727, c:-0.0260	0.9978	0.3920	0.0138	0.00024
	Diffusion approach	a:-129.3512, k:0.2789, b:0.9962	0.9986	0.2860	0.0112	0.00015
70	Henderson and Pabis	a:1.0215, k:0.2252	0.9934	0.9071	0.0261	0.00085
	Lewis	k:0.2211	0.9929	0.9004	0.0272	0.00082
	Page	k:0.1621, n:1.1766	0.9980	0.4800	0.0146	0.00026
	Two term exponential	a_1:0.5205, k_1:0.2252, a_2:0.5011, k_2:0.2252	0.9070 0.9934	0.0261	0.00114	
	Logarithmic	a:1.0614, k:0.1948, c:-0.0539	0.9983	0.4430	0.0133	0.00025
	Diffusion approach	a:-145.4271, k:0.3509, b:0.9962	0.9981	0.4660	0.0140	0.00028
80	Henderson and Pabis	a:1.0186, k:0.2566	0.9934	1.0531	0.0271	0.00098
	Lewis	k:0.2525	0.9929	1.0180	0.0280	0.00090
	Page	k:0.1880, n:1.1823	0.9981	0.5320	0.0146	0.00043
	Two term exponential	a_1:0.5187, k_1:0.2566, a_2:0.4999, k_2:0.2566	0.9934	1.0500	0.0271	0.00148
	Logarithmic	a:1.0732, k:0.2157, c:-0.0686	0.9988	0.0371	0.0114	0.00020
	Diffusion approach	a:-148.5126, k:0.4034, b:0.9962	0.9982	0.5230	0.0142	0.00032

Table 3. Statistical results obtained from the six selected drying models and estimate parameters for agave slabs treated

Temperature (°C)	Models	Model constants	R^2	EMD (%)	ERMS	χ^2
50	Henderson and Pabis	a:1.0119, k:0.1446	0.9977	0.3090	0.0016	0.00014
	Lewis	k:0.1430	0.9976	0.3170	0.0016	0.00021
	Page	k:0.1221, n:1.0718	0.9987	0.2350	0.0009	0.00011
	Two term exponential	a_1:0.5087, k_1:0.1446, a_2:0.5032, k_2:0.1446	0.9977	0.3090	0.0016	0.00019
	Logarithmic	a:1.0244, k:0.1347, c:-0.0227	0.9989	0.3170	0.0016	0.00021
	Diffusion approach	a:-112.9512, k:0.1971, b:0.9969	0.9994	0.2070	0.0008	0.00009
60	Henderson and Pabis	a:1.0177, k:0.1877	0.9966	0.4911	0.0173	0.00032
	Lewis	k:0.1847	0.9962	0.4954	0.0181	0.00035
	Page	k:0.1469, n:1.1181	0.9987	0.2822	0.0108	0.00012
	Two term exponential	a_1:0.5144, k_1:0.1877, a_2:0.5033, k_2:0.1877	0.9966	0.4911	0.0173	0.00032
	Logarithmic	a:1.0327, k:0.1746, c:-0.0.0238	0.9985	0.4954	0.0113	0.00013
	Diffusion approach	a:-135.3750, k:0.2736, b:0.9967	0.9989	0.2598	0.0099	0.00010
70	Henderson and Pabis	a:1.0228, k:0.2200	0.9940	0.8300	0.0247	0.00067
	Lewis	k:0.2157	0.9934	0.8270	0.0258	0.00073
	Page	k:0.1576, n:1.1761	0.9983	0.4010	0.0130	0.00018
	Two term exponential	a_1:0.5208, k_1:0.2200, a_2:0.5020, k_2:0.2200	0.9940	0.8300	0.0247	0.00062
	Logarithmic	a:1.0536, k:0.1952, c:-0.0429	0.9979	0.4710	0.0146	0.00023
	Diffusion approach	a:-182.6784, k:0.3426, b:0.9970	0.9984	0.3890	0.0126	0.00017
80	Henderson and Pabis	a:1.0216, k:0.2590	0.9931	1.0610	0.0274	0.00084
	Lewis	k:0.2543	0.9926	1.0282	0.0285	0.00093
	Page	k:0.1824, n:1.2052	0.9985	0.4589	0.0128	0.00018
	Two term exponential	a_1:0.5220, k_1:0.2590, a_2:0.4996, k_2:0.2590	0.9931	0.8616	0.0274	0.00084
	Logarithmic	a:1.0619, k:0.2253, c:-0.0522	0.9979	0.5720	0.0153	0.00026
	Diffusion approach	a:-181.2456, k:0.4157, b:0.9967	0.9985	0.4637	0.0127	0.00018

The model selected (Diffusion approach) proved to be adequate to describe the drying behavior of agave slabs. Thus, the knowledge of drying kinetics and their modeling could be important to design, simulate and optimize drying process and the information obtained from drying models can be apply to estimate optimum drying conditions.

3.3 Effective moisture diffusivity (D_{eff}) and activation energy (E_a)

As the results showed that the drying of UT and T agave slabs occurs in the falling rate period and the moisture transfer during drying is controlled by internal diffusion, the experimental required data for the determination of diffusivity coefficients can be determined by means of the Fick's diffusion equation. The linear regressions of ln (MR) against drying time are presented in Figure 4a and 4b. The slope derived from linear regression allows obtaining the values of the effective moisture diffusivity (D_{eff}). Generally, the D_{eff} is used as a consequence of scarce information on the mechanism of moisture transfer during drying and complexity of the process (Kashaninejad *et al*., 2007). The average values of effective moisture diffusivity (D_{eff}) at different drying temperature for UT and T agave slabs can be observed in Table 4, where the D_{eff} varied from 3.73×10^{-9} $m^2s^{-1}$to 6.99×10^{-9}, for the case of UT agave slabs and from 3.65×10^{-9} $m^2s^{-1}$to $7.74\times10^{-9}$for T agave slabs. As expected, the values of D_{eff} increased with increasing temperature and were in the suitable general range of 10^{-9} to 10^{-8} $m^2s^{-1}$for drying of the biological materials; this effect has been reported for heterogeneous systems, included vegetable tissues (Chen *et al*., 2012; Shen *et al*., 2011; Ruiz *et al*., 2008; Sacilik *et al*., 2007; Doymaz, 2005; Doulia *et al*., 2000). It can be seen, that the drying at 50, 60 and 70 °C for UT agave slabs promoted a slightly increase on the values of the effective diffusivity coefficients in comparison with T samples. Frequently, for the drying of biological materials, it has been reported that the pretreatment by dipping with several chemical compounds such as alkali solutions, oils, fatty acid ethyl esters, organic acids, inorganic salts, combined with thermal treatment as the blanching, can increase the effective moisture diffusivity reducing the drying time by relaxing tissue structure, removal of film wax or polymeric compounds on the vegetal tissue (Walde *et al*., 2006; Doymaz, 2006, 2010; Tarhan, 2007; Vásquez-Parra *et al*., 2013). However, the pretreatment with hydrochloric acid did not increase the values of effective moisture diffusivity, when the samples were dried at 50, 60 and 70 °C, probably due to that acid treatment could promote a decrease on the permeability of agave tissue structure. A proposal to explain this effect is that under acid conditions and without blanching, a partial solubilization of some structural components, as the cellulose, hemicellulose and lignin, could have occurred during the chemical pretreatment (Köhlerand Spatz, 2002; Bessadok *et al*., 2009). Subsequently, when the drying proceeds, the temperature and internal stresses in the sample are increased, at the same time, the fast drying leads

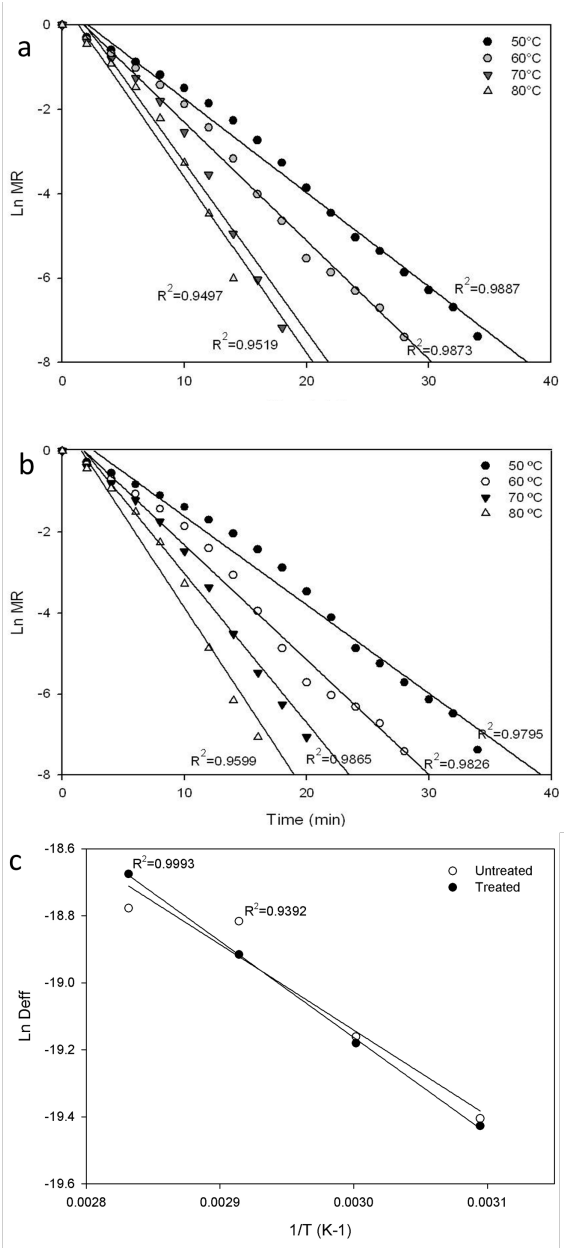

Fig. 4. a) Experimental logarithmic moisture ratio (MR) in function drying time at different drying temperatures for agave slabs untreated and b) treated. c) Arrhenius-type relationship between the logarithm of effective moisture diffusivity (D_{eff}) and the inverse of absolute temperature for agave slabs untreated and treated.

Table 4. Drying parameters values of agave slabs untreated and treated at different drying conditions.

Treatment	Temperature	D_{eff} (m^2/s)	D_o (m^2/s)	E_a (kJ/mol)
Agave slabs untreated	50°C	3.73×10^{-9} (R^2=0.99)	1.03×10^{-5}	21.22
	60°C	4.76×10^{-9} (R^2=0.99)		
	70°C	6.72×10^{-9} (R^2=0.95)		
	80°C	6.99×10^{-9} (R^2=0.95)		
Agave slabs treated	50°C	3.65×10^{-9} (R^2=0.98)	2.64×10^{-5}	23.89
	60°C	4.67×10^{-9} (R^2=0.98)		
	70°C	6.09×10^{-9} (R^2=0.99)		
	80°C	7.74×10^{-9} (R^2=0.96)		

to a mechanical stabilization of the surface, and a thin crust or shell in the external surface of slabs can be formed, promoting a diminishing on the water diffusion rate (Sturm *et al*., 2014; Mayor and Sereno, 2004). In contrast, for the drying at 80 °C the water diffusion rate was increased for T samples in comparison with UT slabs. This could be due to a high drying temperature avoiding the formation of crust or its disruption by an effect of melting or plasticization of the compounds structural and polymeric of agave tissue. Consequently, the water transport can be facilitated under high drying temperature, maybe due to the drying temperature is close to boiling temperature of water and in consequence the water diffusion that could be carried out in vapor phase.

Additionally, the effective moisture diffusivity can be associated with drying temperature by using Arrhenius-type relationship to obtain the activation energy (E_a). The E_a is the energy barrier that must be overcome in order to activate moisture diffusion and the diffusivity constant equivalent (D_o) to the diffusivity at infinitely high temperature (Arabhosseini *et al*., 2009; Wang *et al*., 2007). Thus, the logarithm of D_{eff} as a function of the reciprocal of the absolute temperature (Figure 4c) for UT and T agave slabs results in a linear relationship with a R^2 of 0.94 and 0.99 respectively. The diffusivity constant (D_o) and activation energy (E_a), values are shown in Table 4. From the slope of the curve, the values of activation energy obtained were: 21.22 and 23.89 kJ/mol for UT and T agave slabs respectively. The E_a values found for agave slabs were in reasonable agreement with the data reported by several authors for different biological materials (Gazor and Mohsenimanesh, 2010; Vega *et al*., 2010; Guíne and Fernández, 2006; Senadeera *et al*., 2003). High values of the activation energy are associated with materials where the water is bound more strongly or samples having a dense structure. Thereby, for treated agave slabs the activation energy was slightly larger than untreated agave slabs, maybe due to the formation of the crust caused by acid treatment when the slabs are dried at 50, 60 and 70 °C. The equations 11 and 12 show the effect of temperature on the D_{eff} of untreated and treated agave slabs respectively, as they are useful for the design and scale of equipment in the temperature range studied.

$$D_{eff} = 1.03\times10^{-5}\exp\left(-\frac{2553.27}{T}\right) \quad (12)$$

$$D_{eff} = 2.64\times10^{-5}\exp\left(-\frac{2873.81}{T}\right) \quad (13)$$

3.4 Microstructure and shrinkage

The microstructure of agave slabs observed under ESEM is shown in the Figure 5. Fresh tissue of UT samples displayed intact cells with a regular and isodiametric shape, with typical structure of parenchymatic tissue and also an opaque aspect; cell walls with thick borders, turgid cells and filled with intracellular material could be perceived. However, the acid treatment caused changes in the microstructure of agave tissue and although the cells of treated fresh samples conserved its regular and isodiametric shape, the cellular walls showed thin borders, tissue with a translucent aspect and cells empty without intracellular material. In the case of the dried samples, the T agave slabs showed a more structural damage than UT samples, mainly in the T samples at 70°C, where it can be observed a high loss of cellular shape, severe structural damage with great number of cells melted and breached.

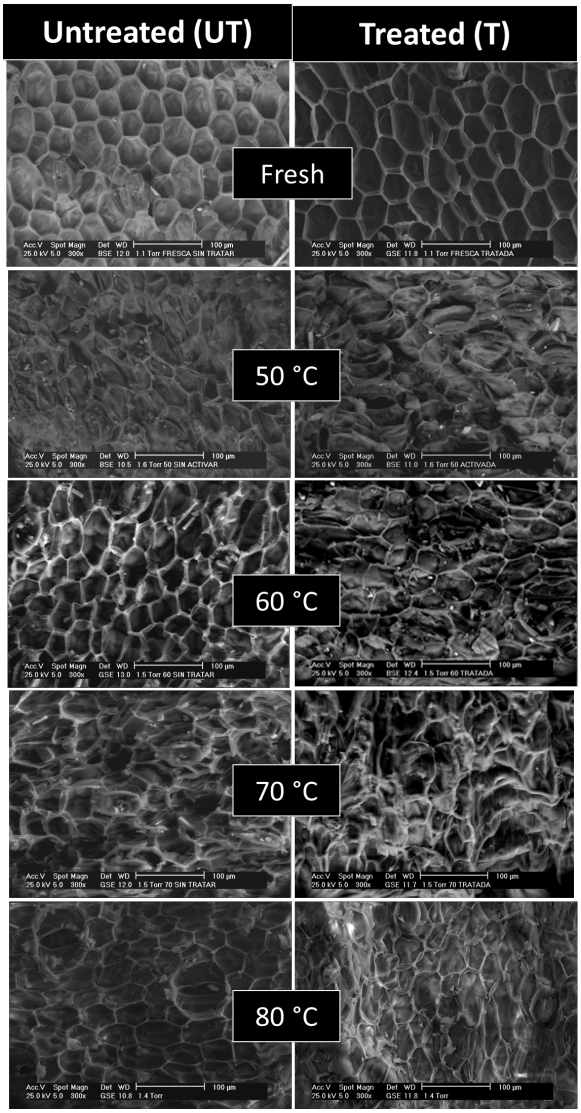

Fig. 5. Environmental scanning electron microscopy micrographs of agave epidermis slabs, fresh and drying at different temperatures, untreated and treated samples.

In this way, microstructural changes caused by pretreatment promoted a large collapsing and deformation of the cells on the slabs surface that probably can explain the low rate of drying observed in the T samples dried at 50-70 °C. When drying at 80 °C, the collapsing, damaging and crumpling of cells were more noticeable for T samples in comparison with UT samples, although some isodiametric shape of cells can be still observed; maybe due to that at this temperature the drying was fast and water diffusion could take place in vapor phase. Additionally, as drying at 80 °C for T samples was carried out at higher rate, a less cellular damage could observed in contrast with T samples drying at 70 °C, in this temperature cellular damage was the more drastic in comparison with the others drying conditions. The drying temperature effect on the microstructure of biological materials has been previously documented and the our results are in agreement with those reported for SEM images of apple slices, carrot cubes, *Aloe vera* gel slabs and agave slabs, dried at a temperature range of 40-80 °C (Vega-Gálvez *et al*., 2012; Sansiribhan *et al*., 2012; Gumeta *et al*., 2011; Miranda *et al*., 2010).The effect of pretreatments by dipping in boiling water, vacuum impregnation, freezing/thawing, and uni-axial compression on the apple microstructure has been reported to damage the tissue structure, yielding larger cell cavities and caused higher drying rates and diffusivity coefficients (Ramírez *et al*., 2011). While, Maldonado *et al*., (2010) has reported a great cellular damage, absence of middle lamella and plasmolysis in mango osmodehydrated and pretreated with sucrose and glucose. However, there are not reports about the effect of pretreatment with hydrochloric acid and convective drying on the microstructure of Agave epidermis.

In overall, the relative shrinkage was higher for UT samples than for T samples and in both cases the percentage of shrinkage increased in relation to drying temperature (Figure 5a). Multiple comparison test showed that the shrinkage (%) of UT samples at 50 °C had significant difference in relation with the other drying temperatures, while the samples at 60 °C and 80 °C, also showed statistical difference between them. In the case of T samples dried at 50 °C and 60 °C, the shrinkage (%) had significant differences with the samples at 70 and 80 °C. While, in the comparison the shrinkage between the UT and T samples, only the samples dried at 60 °C and 80 °C have statistical different. As it has been aforementioned, the acid treatment could promote a decrease on the permeability of agave surface by means of a partial solubilization of the structural components such as cellulose, hemicellulose and lignin (Köhler and Spatz, 2002; Bessadok *et al*., 2009), forming a small crust in the surface of T samples, and higher damage in cellular structure as was observed under ESEM. This could explain the less shrinkage observed in the agave samples treated with acid. In relation to the dependence of the shrinkage with drying temperature, the effect the drying temperature on the shrinkage is mainly due to higher drying rate when the temperature is increased. This effect has been reported for biological materials such as

apples, carrots and potatoes (Vega-Gálvez *et al*., 2012; Sansiribhan *et al*., 2012; Sturm *et al*., 2014; Mayor and Sereno, 2004).

3.5 Biosorption capability of Pb^{+2}

In this work, the combine effect of an acid pretreatment and fluidized bed drying temperatures on the biosorption capability of Pb^{+2} of agave epidermis slabs was studied. Frequently, the biological samples used in biosorption experiments are initially preconditioned by means of acid treatment by dipping the materials into HCl or HNO_3, and then drying over a wide range of temperature conditions (40-110 °C) (Mata *et al*., 2009; Qi and Aldrich, 2008; Schiewer and Balaria 2009; Njikam and Schiewer, 2012). These drying temperatures are typically used in the standard methods for the determinations of the moisture contain and preparation biosorbent materials. However, the combined effect of the acid pretreatment and the drying temperature have been scarcely studied. For instance, the effectiveness of biosorbents depends on a large extent on their biochemical composition, particularly their functional groups, where carboxyl groups play an important role in metal biosorption of several biomaterials, such as pectin, cellulose, hemicellulose and lignin, besides the ability of some of them, to bind divalent cations (Schiewer and Balaria, 2009); Nevertheless, these components could be lixiviated or modified by the acid treatments or drying process. Moreover, during drying, the biomaterial microstructure is drastically affected. This promotes changes in their superficial area and permeability, which have been related to heavy metal biosorption capability. One non exploited waste biomaterial, that could be used in biosorption of heavy metals, due to its structural components is agave. Figure 5b shows that the Pb^{+2} biosorption capability of fresh UT samples was higher than fresh T samples ($p < 0.05$). Similar behavior was observed between the samples UT and T dried at 80 °C. While for UT and T samples dried at 70 °C there was not significant differences. This behavior could be due to two phenomena, in the case fresh samples the acid treatment could have lixiviated some structural components and this modified the content of the carboxyl groups involved in the biosorption. In the case of dry samples, the high drying temperatures applied (80 °C) could promote changes in the superficial area, microstructure and shrinkage, that caused a reduction on the biosorption capability of Pb^{+2} on the biomaterial. These modifications on the sample surface could

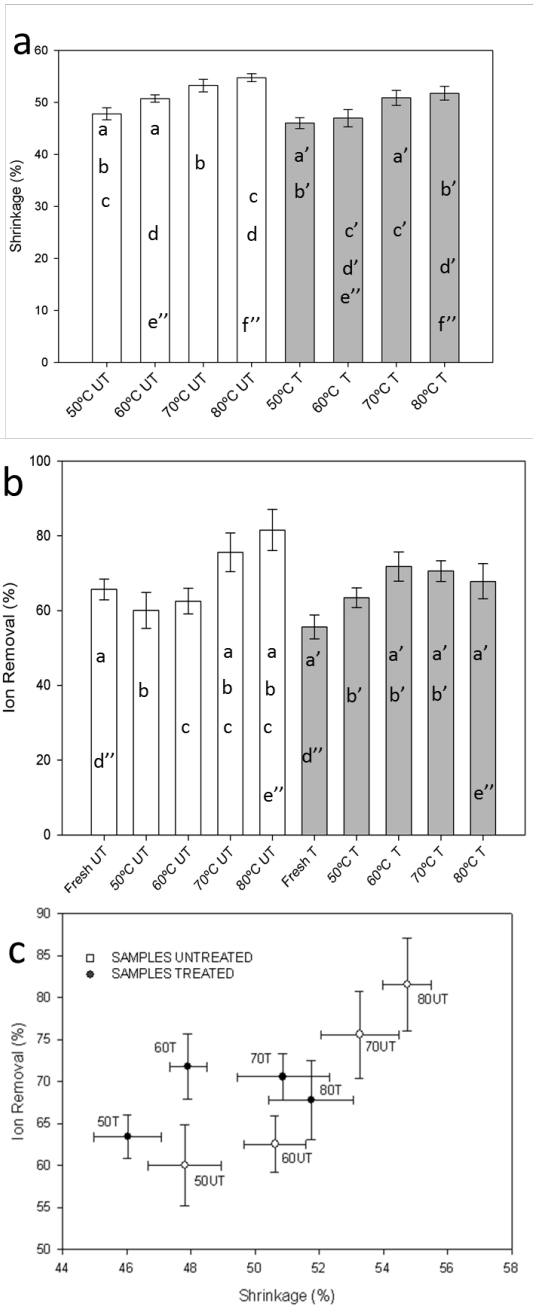

Fig. 6. a) Effect of treatment conditions on the % shrinkage, b) effect treatment conditions on the % ion removal (Pb^{+2}) and c) relationship between % shrinkage and % ion removal. UT: Untreated samples and T: Treated samples. Same letters in the each plot indicate significant difference ($p \leq 0.05$). ' indicate comparison between T samples. " Indicate comparison between UT and T samples at same temperature or treatment.

be due to reactions between the functional groups of biopolymeric compounds associated with the biosorption, that could be catalyzed by the protonation of biomaterial and a partial hydrolysis of some structural components of the agave tissue, and this could have blocked some active carboxyl groups useful for the biosorption.

When only the effect of drying temperature on the biosorption capability of Pb^{+2} was compared, significant variations between UT and T samples dried at different temperatures (Figure 5b) were found. Differences ($p < 0.05$) between UT samples, fresh and dried at 50 °C and 60 °C in comparison with the dry material at 70 °C and 80 °C were observed. In the case of T samples, the behavior was similar, and significant differences were detected for fresh and dry materials at 50 °C in comparison with the dry samples at 60 °C, 70 °C and 80 °C, and 60 °C and 70 °C respectively. For UT and T samples, the increase of temperature and a higher drying rate caused an slight improvement on the biosorption capability of Pb^{+2}; this can be linked to an increase in the superficial area, a higher damage on the microstructure and a large shrinkage in the biomaterial.

Finally, the relationship between the biosorption capability of Pb^{+2} and the shrinkage is shown in the Figure 6c, where for UT samples there is a clear tendency to increase the heavy metal biosorption capability with relation to increase of shrinkage degree and drying temperature. While, for T samples the biosorption capability did not show a clear tendency to increasing with relation the shrinkage. At low temperatures (50 °C and 60 °C) biosorption capability was greater than UT dry samples processed at the same temperatures, but at high temperatures (70 °C and 80 °C) the biosorption decrease in comparison with UT samples. As has been explained above this reduction of the biosorption capability can be associated to the lixiviation of biopolymers and the blocked of functional groups available for the biosorption. Thus, the UT samples drying at 70 °C and 80 °C were the better conditions for the biosorption of Pb^{+2}, suggesting that the acid pretreatment for activation of the biomaterial surface could not be favorable, when the shrinkage is drastic.

Conclusions

On the basis of obtained results it can be concluded that:

1. Drying air temperature had significant effect on the moisture ratio of the samples, internal water diffusion controlled the fluidized bed drying of UT and T agave and Diffusion approach model showed the best fitting for drying kinetics.

2. The effective diffusivity varied from 3.73×10^{-9} to 6.99×10^{-9} m^2s^{-1}, for UT agave slabs and from 3.65×10^{-9} to 7.74×10^{-9} m^2s^{-1} for T agave slabs. The activation energy was found to be 21.22 and 23.89 kJ/mol for UT and T samples respectively.

3. ESEM studies indicated that the acid pretreatment modified the microstructure of agave tissue. As a result, the T agave slabs showed a more microstructural damage than the UT samples, mainly for the T samples dried at 70°C, where the largest cellular damage and a great number of melted and ruptured cells were observed. Shrinkage was higher for the UT samples than the T samples, and in both cases the shrinkage (%) was increased in relation to drying temperature. Acid pretreatment caused solubilization and lixiviation of some structural components on the slabs surface that promoted the formation of a crust that could explain the lower shrinkage and great microstructural damage observed.

4. Treated and dried samples at 70 and 80 °C showed a reduction in their Pb^{+2} biosorption capability caused by a large shrinkage and severe microstructural changes, that could have blocked the carboxyl groups associated with the biosorption phenomenon. While for UT samples their biosorption capability was increased in relation with the increase of the shrinkage and drying temperature. As a recommendation for biosorbents preparation, the treated and dried samples at low temperatures (50 and 60 °C) can improve their biosorption capability, while for UT samples the application of higher drying temperatures (70 and 80 °C) improve the biosorption capability.

5. The results found in this work could be useful to design, simulate, and scale drying equipment and also to provide criteria for the selection of pretreatment conditions and drying for preparation of biosorbents for Pb^{+2} from agave wastes.

Acknowledgments

Mayuric Teresa Hernández Botello wishes to thank CONACyT for the scholarship provided for her studies and international stay. This research was funded through projects 20110627 and 20121001, 20120789, 20130333 and 20140387 at the Instituto Politécnico Nacional (SIP-IPN Mexico) and133102 of CONACyT

Nomenclature

a	fit coefficient, -
a_1	fit coefficient, -
a_2	fit coefficient, -
B	fit coefficient, -
C	model constant, -
C	concentration, ppm
CI	current intensity, ampers
C_i	initial concentration of Pb^{+2}, ppm
C_f	final concentration of Pb^{+2}, ppm
Cu	cuticle
d.b.	dry basis
D_{eff}	effective diffusivity, m^2s^{-1}
D_o	pre-exponential factor m^2s^{-1}
DR	drying rate, g (water) g^{-1}(dry solids) min^{-1}
E_a	energy activation, $kJmol^{-1}$
Ec	epidermis cells
E_{MD}	relative percent deviation, -
Ep	epidermis of agave
E_{RMS}	root mean square error, -
ESEM	environmental scanning electron microscopy
GSE	gaseous detector of secondary electrons
k	model constant (s^{-1})
k_1	model constant (s^{-1})
k_2	model constant (s^{-1})
L	half of thickness of slab, m
M_1	moisture content at time t_1, g (water) g^{-1}(dry solids)
M_2	moisture content at time t_2, g (water) g^{-1}(dry solids)
M_e	equilibrium moisture content, g (water) g^{-1}(dry solids)
M_o	initial moisture content, g (water) g^{-1}(dry solids)
MR	moisture ratio
$M_{R,exp,I}$	experimental dimensionless moisture ratio
$M_{R,pre,I}$	predicted dimensionless moisture ratio
M_t	moisture content at time t, g (water) g^{-1}(dry solids)
N	model constant -
N	number of observations
Pa	parenchyma tissue
R	universal gas constant, 8.314 J $mol^{-1}K^{-1}$
R^2	coefficient of determination
T	treated agave epidermis
t	time, s
T	absolute temperature, K
t_1	drying time at time 1, min
t_2	drying time at time 2, min
UT	untreated agave epidermis
V_i	initial volume, m^3
V_f	final volume, m^3
z	number of constants

References

Abalone, R., Gastón, A., Cassinera, A., Lara, M.A. (2006).Thin layer drying of Amaranth seed. *Biosystems Engineering 93*, 179-188.

Akgun, N., Doymaz I. (2005). Modelling of olive cake thin-layer drying process. *Journal of Food Engineering 68*, 455-461.

Akmel, D.C., Assidjo, N.E., Kouamé, P., Yao, K.B. (2009). Mathematical modeling of sun drying kinetics of thin layer cocoa (*Theobroma cacao*) beans. *Journal of Applied Sciences Research 5*, 1110-1116.

Arabhosseini, A., Huisman, W., van Boxtel, A., Müller, J. (2009). Modeling of thin layer drying of tarragon (*Artemisia dracunculus* L.). *Industrial Crops and Products 29*, 53-59.

Arzate-Vázquez, I., Chanona-Pérez, J.J., Calderón-Domínguez, G., Terres-Rojas. E., Garibay-Febles V., Martínez-Rivas, A., Gutiérrez-López, G.F. (2012). Microstructural characterization of chitosan and alginate films by microscopy techniques and texture image analysis. *Carbohydrate Polymers 87*, 289-299.

Barrozo, M.A.S., Henrique, H.M., Sartori, D.J.M., Freire, J.T. (2006). The use of the orthogonal collocation method on the study of the drying kinetics of soybean seeds. *Journal of Stored Products Research 42*, 348-356.

Bessadok, A., Langevin, D., Gouanvé, F., Chappey, C., Roudesli, S., Marais, S. (2009). Study of water sorption on modified Agave fibres. *Carbohydrate Polymers 76*, 74-85.

Bhainsa, K.C., D'Souza. S.F. (2008). Removal of copper ions by the filamentous fungus, *Rhizopus oryzae* from aqueous solution. *Bioresource Technology 99*, 3829-3835.

Calzetta, A. N. R., Aguerre, R. J., Suarez, C. (2004). Drying characteristics of amaranth grain. *Journal of Food Engineering 65*, 197-203.

Chen, D., Zheng, Y., Zhu, X. (2012). Determination of effective moisture diffusivity and drying kinetics for poplar sawdust by thermogravimetric analysis under isothermal condition. *Bioresource Technology 107*, 451-455.

Chua, K.J., Mujumdar, A.S., Chou, S.K., Hawlader, M.N.A., Ho, J.C. (2000). Convective drying of banana, guava and potato pieces: effect of cyclical variations of air temperature on drying kinetics and color change. *Drying Technology 18*, 907-936.

Cihan, A., Kahveci, K., Hacihafizoglu, O. (2007). Modeling of intermittent drying of thin layer rough rice. *Journal of Food Engineering 79*, 293-298.

Comte, S., Guibaud, G., Baudu, M. (2006). Biosorption properties of extracellular polymeric substances (EPS) resulting from activated sludge according to their type: Soluble or bound. *Process Biochemistry 41*, 815-823.

Comte, S., Guibaud, G., Baudu, M. (2008). Biosorption properties of extracellular polymeric substances (EPS) towards Cd, Cu and Pb for different pH values. *Journal of Hazardous Material 151*, 185-193.

Crank, J. (1975). *The Mathematics of Diffusion*, 2nd ed. Clarendon Press, Oxford, UK.

Demir, V., Gunhan, T., Yagcioglu, A.K. (2007). Mathematical modeling of convection drying of green table olives. *Biosystems Engineering 98*, 47-53.

Doulia, D., Tzia, K., Gekas, V. (2000). A knowledge base for the apparent mass diffusion coefficient (D_{EFF}) of foods. *International Journal of Food Properties 3*, 1-14.

Doymaz I. (2010). Effect of citric acid and blanching pre-treatments on drying and rehydration of Amasya red apples. *Food and Bioproducts Processing 88*, 124-132.

Doymaz, I. (2006). Drying kinetics of black grapes treated with different solutions. *Journal of Food Engineering 76*, 212-217.

Doymaz, I. (2005). Drying behavior of green beans. *Journal of Food Engineering 69*, 161-165.

Doymaz, I. (2011). Drying of green bean and okra under solar energy. *Chemical Industry & Chemical Engineering Quarterly 17*, 199-205.

Evin, D. (2012). Thin layer drying kinetics of *Gundelia tournefortii* L. *Food and Bioproducts Processing 90*, 323-332.

Feng, N., Guo, X., Liang, S., Zhu, Y., Liu, J. (2011). Biosorption of heavy metals from aqueous solutions by chemically modified orange peel. *Journal of Hazardous Materials 185*, 49-54.

Fernandez, L., Castillero, C., Aguilera, J.M. (2005). An application of image analysis to dehydration of apple discs. *Journal of Food Engineering 67*, 185-193.

Gazor, H.R., Mohsenimanesh, A. (2010). Modelling the drying kinetics of canola in fluidized bed dryer. *Czech Journal of Food Sciences 28*, 531-537.

Gely, M.C., Santalla, E.M. (2007). Moisture diffusivity in quinoa (*Chenopodium quinoa* Willd.) seeds: effect of air temperature and initial moisture content of seeds. *Journal of Food Engineering 78*, 1029-1033.

Guiné, R.P.F., Fernández, R.M.C. (2006). Analysis of the drying kinetics of chestnuts. *Journal of Food Engineering 76*, 460-467.

Gumeta-Chávez, C., Chanona-Pérez, J.J., Mendoza-Pérez, J.A., Terrés-Rojas, E., Garibay-Febles, V., Gutiérrez-López, L.G. (2011). Shrinkage and Deformation of Agave atrovirens Karw Tissue during Convective Drying: Influence of Structural Arrangements. *Drying Technology: An International Journal 29*, 612-623.

Iguaz, A., San Martín, M.B., Maté, J.I., Fernández, T., Vírseda, P. (2003). Modelling effective moisture diffusivity of rough rice (*Lido cultivar*) at low drying temperatures. *Journal of Food Engineering 59*, 253-258.

Iñiguez-Covarrubias, G., Díaz-Teres, R., Sanjuan-Dueñas, R., Anzaldo-Hernández, J., Rowell, R.M. (2001). Utilization of by-products from the tequila industry. Part 2: potential value of *Agave tequilana* Weber azul leaves. *Bioresource Technology 77*, 101-108.

Kashaninejad, M., Mortazavi, A., Safekordi, A., Tabil, L.G. (2007). Thin-layer drying characteristics and modeling of pistachio nuts. *Journal of Food Engineering 78*, 98-108.

Kerdpiboon, S., Devahastin, S., Kerr, W.L. (2007). Comparative fractal characterization of physical changes of different food products during drying. *Journal of Food Engineering 83*, 570-580.

Köhler, L., Spatz H.-C. (2002). Micromechanics of plant tissues beyond the linear-elastic range. *Planta 215*, 33-40.

López-García, M., Lodeiro, P., Herrero, R., Sastre de Vicente, M.E. (2012). Cr (VI) removal from synthetic and real wastewaters: The use of the invasive biomass *Sargassum muticum* in batch and column experiments. *Journal of Industrial and Engineering Chemistry 18*, 1370-1376.

Maldonado, S., Arnau, E., Bertuzzi, M.A. (2010). Effect of temperature and pretreatment on water diffusion during rehydration of dehydrated mangoes. *Journal of Food Engineering 96*, 333-341.

Markowski, M., Bialobrzewski, I., Modrzewska, A. (2010). Kinetics of spouted-bed drying of barley: Diffusivities for sphere and ellipsoid. *Journal of Food Engineering 96*, 380-387.

Mata, Y.N., Blázquez, M.L., Ballester, A., González, F., Muñoz, J.A. (2009). Sugar-beet pulp pectin gels as biosorbent for heavy metals: Preparation and determination of biosorption and desorption characteristics. *Chemical Engineering Journal 150*, 289-301.

Mayor, L., Sereno, A.M. (2004). Modelling shrinkage during convective drying of food materials: a review. *Journal of Food Engineering 61*, 373-386.

McLaughlin, C. P., Magee, T.R.A. (1998). The effect of shrinkage during drying of potato spheres and the effect of drying temperature on vitamin C retention. *Food and Bioproducts Processing 76*, 138-142.

Miranda, M., Vega-Gálvez, A., García, P., Di Scala, K., Shi, J., Xue, S., Uribe, E. (2010). Effect of temperature on structural properties of Aloe vera (*Aloe barbadensis* Miller) gel and Weibull distribution for modelling drying process. *Food and Bioproducts Processing 88*, 138-144.

Mohammadi, T., Razmi, A., Sadrzadeh, M. (2004). Effect of operating parameters on Pb^{2+} separation from wastewater using electrodialysis. *Desalination Strategies in South Mediterranean Countries 167*, 379-385.

Niamnuy, C., Devahastin, S. (2005). Drying kinetics and quality of coconut dried in a fluidized bed dryer. *Journal of Food Engineering 66*, 267-271.

Njikam, E., Schieve, S. (2012). Optimization and kinetic modeling of cadmium desorption from citrus peels: A process for biosorbent regeneration. *Journal of Hazardous Materials 213-214*, 242-248.

Perea-Flores, M.J., Chanona-Pérez, J.J., Garibay-Febles,V., Calderón-Domínguez, G., Terrés-Rojas, E., Mendoza-Pérez, J.A., Herrera-Bucio, R. (2011). Microscopy techniques and image analysis for evaluation of some chemical and physical properties and morphological features for seeds of the castor oil plan (*Ricinus communis*). *Industrial Crops and Products 34*, 1057-1065.

Perea-Flores, M.J., Garibay-Febles, Chanona-Pérez, J.J., V., Calderón-Domínguez, G., Méndez-Méndez, J.V., Palacios-González, E., Gutiérrez-López, G.F. (2012). Mathematical modeling of castor oil seeds (*Ricinus communis*) drying kinetics in fluidized bed at high temperatures. *Industrial Crops and Products 38*, 64-71.

Promvonge, P., Boonloi, A., Pimsarn, M., Thianpong, Ch. (2011). Drying characteristics of peppercorns in a rectangular fluidized-bed with triangular wavy walls. *International*

Communications in Heat and Mass Transfer 38, 1239-1246.

Qi, B.C., Aldrich, C. (2008). Biosorption of Heavy metals from aqueous solutions with tobacco dust. *Bioresource Technology 99*, 5596-5601.

Rafiee, S.H., Keyhani, A., Sharifi, M., Jafari, A., Mobli, H., Tabatabaeefar, A. (2009). Thin layer drying properties of soybean (*Viliamz Cultivar*). *Journal of Agricultural Science and Technology 11*, 289-300.

Ramírez, C., Troncoso E., Muñoz J., Aguilera J. M. (2011). Microstructure analysis on pre-treated apple slices and its effect on water release during air drying. *Journal of Food Engineering 106*, 253-261.

Roberts, J.S., Kidd, D.R., Padilla-Zakour, O. (2008). Drying kinetics of grape seed. *Journal of Food Engineering 89*, 450-455.

Romero-González. J., Gardea-Torresdey, J.L., Peralta-Videa, J.R., Rodríguez, E. (2005). Determination of Equilibrium and Kinetic Parameters of the Adsorption of Cr (III) and Cr (VI) from Aqueous Solutions to *Agave Lechugilla* Biomass. *Bioinorganic Chemistry and Applications 3*, 55-68.

Ruiz-López, I.I., Martínez-Sánchez, C.E., Cobos-Vivaldo, R., Herman-Lara, E. (2008). Mathematical modeling and simulation of batch with airflow reversal. *Journal of Food Engineering 89*, 310-318.

Sacilik, K. (2007). Effect of drying methods on thin-layer drying characteristics of hull-less seed pumpkin (*Cucurbita pepo* L.). *Journal of Food Engineering 79*, 23-30.

Sacilik, K., Elicin, A. K., Unal, G. (2006). Drying Kinetics of Üryani plum in a convective hot-air dryer. *Journal of Food Engineering 76*, 362-368.

Sansiribhan, S., Devahastin, S., Soponronnarit, S. (2012). Generalized microstructural change and structure-quality indicators of a food product undergoing different drying methods and conditions. *Journal of Food Engineering 109*, 148-154

Santiago-Pineda, T., Anaya-Sosa, I., Alamilla-Beltrán, L., Chanona-Pérez, J. J., Gutiérrez-López G. F., Vizcarra-Mendoza, M. (2007). Hidrodynamics and operational parameters of a continuous multistage vertical fluidized bed system. *Revista Mexicana de Ingeniería Química 6*, 59-63.

Schiewer.S. y Balaria, A. (2009). Biosorption of Pb^{+2} by original and protonated citrus peels: Equilibrium, Kinetics, and mechanism. *Chemical Engineering Journal 146*, 211-219.

Senadeera, W., Bhandari, B. R., Young G., Wijesinghe, B. (2003). Influence of shapes of selected vegetable materials on drying kinetics during fluidized bed drying. *Journal of Food Engineering 58*, 277-283.

Shen, F., Peng, L., Zhang, Y., Wu, J., Zhang, X., Yang, G., Peng, H., Qi, H., Deng, S. (2011). Thin layer drying kinetics and quality changes of sweet sorghum stalk for ethanol production as affected by drying temperature. *Industrial Crops and Products 34*, 1588-1594

Shivhare, U.S., Gupta, A., Bawa, A.S., Gupta, P. (2000). Drying characteristics and product quality of okra. *Drying Technology 18*, 409-419

Sirisomboon, P., Kitchaiya, P. (2009). Physical properties of *Jatropha curcas* L. kernels after heat treatments. *Biosystems Engineering 102*, 244-250.

Sturm, B., Nunez, V. A.-M., Hofacker, W. C. (2014). Influence of process control strategies on drying kinetics, colour and shrinkage of air dried apples. *Applied Thermal Engineering 62*, 455-460.

Tarhan, S. (2007). Selection of chemical and thermal pretreatment combination for plum drying at low and moderate drying air temperatures. *Journal of Food Engineering 79*, 255-260.

Vagenas, G.K and Karathanos, V.T. (1993). Prediction of the effective moisture diffusivity in gelatinized food systems. *Journal of Food Engineering 18*, 159-179

Vásquez-Parra, J. E., Ochoa-Martínez, C.I., Bustos-Parra, M. (2013). Effect of chemical and physical pretreatments on the convective drying of cape gooseberry fruits (*Physalis peruviana*). *Journal of Food Engineering 119*, 648-654.

Vega, G.A., Miranda, M., Puente, L., Lopez, L., Rodriguez, K. (2010). Effective moisture diffusivity determination and mathematical modelling of drying curves of the olive-waste cake. *Bioresource Technology 101*, 7265-7270.

Vega-Gálvez, A., Ah-Hen, K. Chacana, M., Vergara J., Martínez-Monzó, J., García-Segovia, P., Lemus-Mondaca, R., Di Scalae, K. (2012). Effect of temperature and air velocity on drying kinetics, antioxidant capacity, total phenolic content, colour, texture and microstructure of apple (var. Granny Smith) slices. *Food Chemistry 132*, 51-59.

Velazquez-Jimenez, Litza H., Pavlick, Andrea., Rangel-Mendez, J. Rene. (2013). Chemical characterization of raw and treated agave bagasse and its potential as adsorbent of metal cations from water. *Industrial Crops and Products 43*, 200-206.

Walde, S.G., Velu, V., Jyothirmayi, T., Math, R.G. (2006). Effects of pretreatments and drying methods on dehydration of mushroom. *Journal of Food Engineering 74*, 108-115.

Wang, Z., Sun, J., Liao, X., Chen, F., Zhao, G. (2007). Mathematical modeling on hot air drying of thin layer apple pomace. *Food Research International 40*, 39-46.